Sistemasi: Jurnal Sistem Informasi
Volume 13, Nomor 6, 2024: 2348-2358

ISSN:2302-8149
e-ISSN:2540-9719

Enhanced Brain Tumor Classification Through Gamma Correction in Deep Learning

[1]Muhammad Naufal*, [2]Harun Al Azies, [3]Rivaldo Mersis Brilianto
[1,2]Study Program in Informatics Engineering, Faculty of Computer Science,
Universitas Dian Nuswantoro, 50131, Semarang, Indonesia
[3]School of Mechanical Engineering, Pusan National University, 2, Busandaehak-ro 63beon-gil,
Geumjeong-gu, 46241, Busan, Republic of Korea
*e-mail: m.naufal@dsn.dinus.ac.id

(***received***: 13 August 2024, ***revised***: 26 September 2024, ***accepted***: 18 October 2024)

Abstract

Classification of brain tumors is a problem in computer-aided diagnosis (CAD). This study classifies three classes of brain tumors: gliomas, meningiomas, and pituitary tumors. Image enhancement is useful for improving the quality of images to be recognized by Computer-Aided Diagnosis (CAD) systems. Gamma correction is one spatial method aimed at manipulating contrast. This method operates with a spatial approach and has relatively low computational time but yields satisfactory results in certain cases. This research compares Gamma Correction with Convolutional Neural Network (CNN) in the classification of brain tumor types. The CNN method without Gamma Correction achieves an accuracy of 86.52%, precision of 83.63%, sensitivity of 86.11%, and specificity of 93.27%. The application of Gamma Correction at 1.5 results in improved performance with an accuracy of 88.80%, precision of 86.49%, sensitivity of 88.06%, and specificity of 94.50%. Meanwhile, Gamma Correction at 0.5 shows an accuracy of 88.59%, precision of 87.59%, sensitivity of 86.68%, and specificity of 94.17%. Overall, the implementation of Gamma Correction in the classification of brain tumor types successfully enhances the CNN classification performance in terms of precision, sensitivity, and specificity compared to without its use.

Keywords: brain tumor, convolutional neural network, gamma correction, image enhancement

1 Introduction

A brain tumor is a disease that occurs due to the presence of abnormal cells in the brain that grow unnaturally. The size, distribution, and shape of the tumor can vary. Brain tumors are categorized into two main types, namely benign tumors and malignant tumors [1]. Benign tumors are tumors that grow slowly, do not have cancer cells, and do not damage the surrounding tissue. Malignant tumors are the opposite of benign tumors, where these tumors contain dangerous cancer cells that can threaten sufferers of this tumor by attacking the surrounding brain tissue and growing rapidly [2]. Cancer is a disease that causes high death rates in the world.

Magnetic resonance imaging (MRI) examination can detect brain tumors. However, the intricacy of the human brain's anatomy makes examination complicated and time-consuming. The sooner a patient is treated, the sooner the treatment will be carried out, and the longer the patient's life expectancy. As a result, MRI images must be identified so that they can aid in patient diagnosis. Many researchers have developed computer-based automatic identification techniques, or CAD [3], [4], [5], to assist neuro-oncologists in analyzing the results of MRI photos, such as tumor detection (segmentation), tumor classification, and determining the stage of tumors in the brain.

Various methodologies and algorithms, such as the deep convolutional neural network (CNN), Bayesian classifier, genetic algorithm, watershed, support vector machine (SVM) approach, and others, have also been created to aid in the categorization of brain tumors based on MRI brain results. A lot is still being developed [6]. The CNN model, for example, has been widely developed and utilized since the ImageNet competition in 2012. Image enhancement is critical for increasing image quality and color correction. By altering the dynamic range of picture pixel intensity distribution, all approaches strive to improve image quality and contrast to enable better interpretation. Fusion-based picture enhancement solutions include merging exposure intensity levels to overcome constraints caused by local modifications. Algorithms include principal component analysis (PCA) and wavelet transform.

ISSN:2302-8149
e-ISSN:2540-9719

Meanwhile, the spatial domain is a method that focuses on histogram-based methods, using algorithms such as histogram equalization, gamma correction, filtering, and thresholding [7]. Gamma correction improves visual representation and image contrast by adjusting the light intensity in the image [8].

The spatial domain offers advantages over fusion-based approaches in that it is simpler, the findings are easier to interpret, it provides local control over pixels, which is a drawback of fusion-based methods, and it has faster computing [7], [8]. As a result, the purpose of this work is to undertake a comparative analysis of the use of gamma correction in CNNs. Researchers anticipate that this study will yield useful results that will aid radiologists, particularly neuro-oncologists, in classifying anomalies in brain tumors.

This research focuses on enhancing image brightness and contrast by spatially adjusting the intensity levels of each pixel using gamma correction. Gamma correction is applied before the modeling process performed by the CNN classifier. It utilizes a non-linear operation to adjust the overall brightness and contrast of an image. This operation works by globally modifying the intensity levels of each pixel, resulting in low complexity.

2 Literature Review

Convolutional neural network (CNN) models have been developed [9] for the segmentation and classification of benign and malignant tumors, the segmentation of simple brain tumors [10], [11], [12], [13] and then with a deep learning approach, and the classification of tumors and non-tumors [14]. Multiclass classification and CNN technique combinations are also being developed. For example, using a mix of CNN methods and a genetic algorithm, researchers classified cancer stages on brain MRI data into glioma, meningioma, and pituitary tumor types [1].The dataset utilized in this study was gathered from multiple sources and had an accuracy of 90.9% for classifying brain tumor stages and 94.2% for classifying types of abnormalities in the brain other than tumors. Machine learning and deep learning algorithms using a vanilla CNN architecture [1], [15] transfer learning [16], [17] and numerous more feature extraction methods [14], [15] are used. This classification performs pretty well, although it is restricted by computation time and dataset availability.

Several research use image enhancement techniques, such as adaptable Histogram Equalization (HE) [18], [19]. The HE method is employed to equalize the histogram by adjusting the image contrast and distributing the range of intensity levels uniformly. Additionally, the type of HE is Clip Limit Adaptive Histogram equalization (CLAHE) [20], [21], which tries to restrict the amount of image enhancement, in addition to segmentation to enhance CNN findings. On the other hand, the processed image has significant excess brightness, color distortion, and uneven contrast. PCA tries to preserve the image's color and texture while reducing features [21]. CNN fusion methods integrate CNN features to produce enhanced features. representative, manual color balancing and denoising using CBDT [22], Wavelet [23] for noise reduction and high-resolution use, and Anisotropic Diffusion Filter (ADF) [24] removes noise from MRI images while preserving the edges of existing objects, skull stripping, and contrast enhancement. The time-shifting method employs gamma correction on five datasets, yielding the best assessment results in terms of time and performance [8]. Another issue with the preparation procedure is the high computing and storage capacity [25]. Spatial domain-based methods outperform fusion-based methods in terms of computational efficiency [8]. Gamma correction is one of the techniques, which improves image quality by altering contrast while keeping the image's average brightness [26].

Several earlier research has demonstrated that CNN is a reasonably effective method for categorizing objects and applying image augmentation, which can increase image quality with rapid computing. Configuring the extent of the influence of gamma correction on CNN in classifying brain tumors is what is unique or novel in this research.

3 Research Method

This section outlines the research framework, encompassing the stages of analysis starting from the analysis of information from the dataset, including its source, data size, and image dimensions. It then explains the research framework used, encompassing data preparation, preprocessing, data splitting, modeling, and evaluation, all summarized in Figure 2.

A. Dataset and Research Variables

The researchers used a public dataset retrieved from the Fighshare collection [27], which included 3064 T1-CE MRIs from 233 patients with three types of cancers (meningioma, glioma, and pituitary

ISSN:2302-8149
e-ISSN:2540-9719

tumors). The collection contains 708 photos of meningioma (82 patients), 1426 images of glioma (89 patients), and 930 images of pituitary tumor cases (62 individuals). The image format supported is. mat, with image dimensions of 512x512 pixels. The dataset was selected because it has been utilized in several studies [15], [28], [29] and presents unique challenges concerning its characteristics. These challenges include a relatively small sample size and an imbalance in the number of instances per class, which accurately reflects real-world data conditions. Figure 1 shows an example of data from this collection.

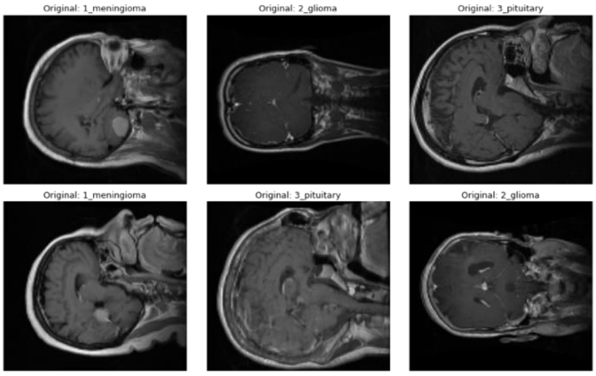

Figure 1. An example of a fighshare collection dataset on three categories of cancer patients

B. Research Framework

The research framework carried out can be seen in Figure 2 below.

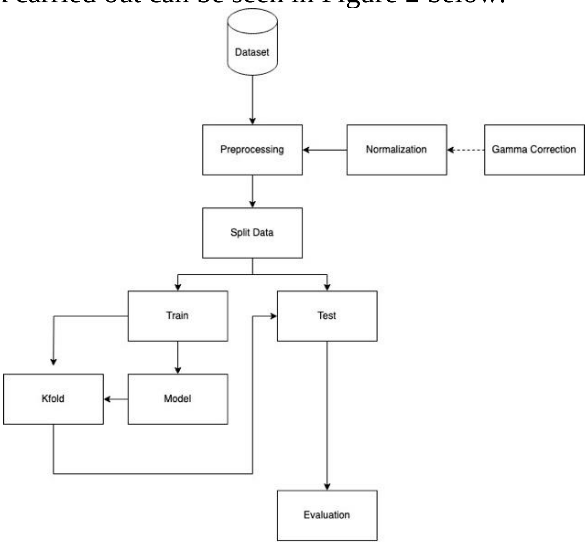

Figure 2. Brain tumor classification research framework

The research workflow begins with preprocessing the input image by scaling it to 224x224 and normalizing it between susceptibility 0 and 1. After that, preprocessing and gamma correction are applied. The data is then randomly divided by the percentage of training and testing to the total number of labels: 70%, and 30%. The data is then categorized using CNN. Model training is done using 5-fold cross-validation. Later, the best fold model will be saved and tested against the test data. A confusion matrix evaluation is performed during the performance evaluation step.

4 Results and Analysis

This section presents a comprehensive evaluation of the research results, examining each stage in detail. The analysis begins by visualizing the impact of gamma correction on the image dataset, showcasing the adjustments in brightness and contrast. The CNN model architecture is then described, highlighting the chosen layers, activation functions, and filter sizes. Finally, the model's performance is evaluated using confussion matrix.

A. Data Preparation

The initial step involves normalizing the input image by adjusting its intensity values to a scale of 0 to 255.0. This normalization process ensures consistency in the image data. Subsequently, the image

 ISSN:2302-8149
e-ISSN:2540-9719

undergoes resizing, where its dimensions are modified to a specific size, transforming it from the original 512x512x3 to 224x224x3. In the experiment, this resizing is crucial for adapting the image to the input requirements of the model under development.

Following resizing, the process incorporates gamma adjustment, a technique employed in image processing to address variations in light intensity perceived by the human eye on different display devices. This correction involves the application of a non-linear function, as depicted in Equation (1), which controls the intensity of light within the image. This step aims to reconcile differences between actual light intensity and the perceptual experience on devices such as computer displays or monitors, thereby enhancing the overall quality of the image in the model's input pipeline [8].

$$Y = \left(\frac{X}{255}\right)^{\gamma} \qquad (1)$$

X is the initial pixel value (in RBG, it ranges from 0-255), and γ is the gamma factor used to adjust the image's contrast and brightness. Meanwhile, Y is the matrix's output value. This equation is used to manage the image's contrast level. When $\gamma = 1$, the image contrast is increased; when $\gamma > 1$, the image contrast is decreased. γ is the exponent value in this formula that regulates how much the intensity level is increased or decreased. Many image processing procedures, notably gamma conversion, assume that the input image has been normalized to the range [0, 1] in float, rather than [0, 255]. The gamma values used are 0.5 and 1.5.

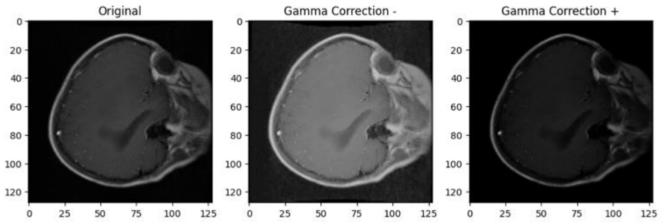

Figure 3. Results of gamma correction treatment

The difference in contrast results before and after gamma correction treatment is shown in Figure 3. A visualization of the image histogram before and after gamma correction is also provided below. The graph in Figure 4. shows a comparison histogram value for image samples without and with gamma correction applied. The gamma value (+) causes more 0 values in pixels, darkening the image, while the gamma correction (-) makes the 0 values less than the original value. The existing data is then segmented into train, test, and validation segments, which account for 70% and 30% of the total data, respectively. The distribution of data was done at random based on the proportion of labels.

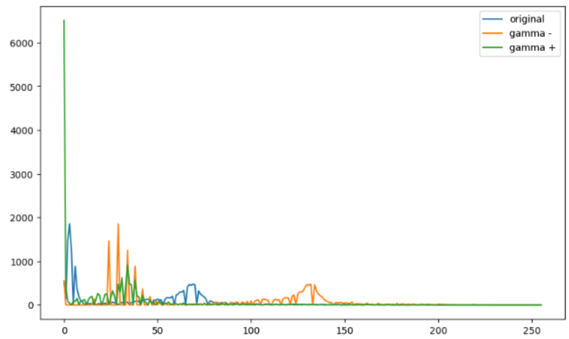

Figure 4. Histogram graph for each treatment

B. Network Architecture

The vanilla CNN employed seeks to use a model with little complexity, therefore the assumption is that when a model like ImageNet is used, it will yield decent results as well. The CNN architecture that was built is seen below.

ISSN:2302-8149
e-ISSN:2540-9719

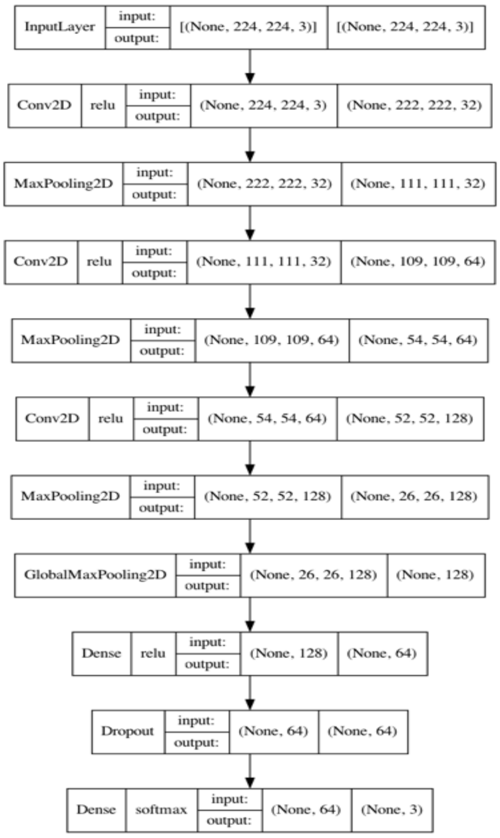

Figure 5. CNN architecture proposed in brain tumor classification research

The network design is shown in Figure 5 to be made up of 32, 64, and 128 consecutive convolutions. Each network is given max-pooling to decrease the number of features produced by each convolution. Then, using global max-pooling, a fully connected layer of 64 layers with a dropout of 0.5 is built before entering the classification layer, followed by a classification layer with soft-max probability and an output of 3. There are a total of 101,699 parameters in this architecture. The batch size value is 32, and the epoch value is 20 for the parameters used.

C. Adam (Adaptive Moment Estimation)

Adam is an adaptive estimating stochastic gradient descent algorithm. In the domain of neural network model training, Adam has various advantages over other optimizers [30]. For starters, Adam is highly adaptable because it automatically adjusts the learning rate for each parameter, allowing for flexible handling of diverse types of data and models. Second, this method is effective at predicting the first (gradient) and second (square of the gradient), which improves optimization efficiency. Third, Adam excels at non-stationary data or distributions that fluctuate over time. Fourth, this optimizer contains regulation settings that can be modified to meet specific needs. Finally, Adam is compatible with a wide range of models and architectures, making it a popular choice for neural network model training. However, optimizer performance might vary based on the dataset and task, therefore it is best to experiment with multiple optimizers to discover the one that best meets your needs. Adam updates the parameters by merging the first and second moments of the gradient. The following equation (2-6) shows Adam's calculation:

$$m1 = beta1 \times m1 + (1 - beta1)\, x\, gradient \quad (2)$$

$$m2 = beta2 \times m2 + (1 - beta2)\, x\, gradient \quad (3)$$

$$m1_{hat} = m1 \div (1 - beta1^{t}) \quad (4)$$

$$m2_{hat} = m2 \div (1 - beta2^{t}) \quad (5)$$

$$p = p - lr\, x\, m1_{hat} \div \left(\sqrt{m2_{hat} + epsilon}\right) \quad (6)$$

Where m represents momentum, beta represents the recurrence parameter, gradient represents the gradient of the parameter's loss function, p represents the parameter, t represents the iteration, lr represents the learning rate, and epsilon is a small number to avoid division by zero. The following

ISSN:2302-8149
e-ISSN:2540-9719

values are employed in this study: learning rate = 0.001, epsilon = 1e-07, beta 1 = 0.9, and beta 2 = 0.999.

D. L2 Kernel Regularizers

The L2 kernel regularizer attempts to reduce overfitting [30] in neural network models by penalizing weights with large values. During model training, L2 works in the context of kernel regularizers by adding the sum of the squares of all weights as part of the loss function. The L2 formula is shown in the following equation (7).

$$L_n = L_0 + \left(\frac{\lambda}{2} \sum i \; \| W_i \|_2^2\right) \qquad (7)$$

If W is a set of kernel weights, L_n is the new loss function, and L_0 is the original loss function. In this case, λ is a penalty parameter that governs how much regularisation affects the loss function. Meanwhile, the λ value that is being used is 0.01. L2 encourages the model to choose smaller weights overall, which can assist in preventing overfitting by reducing model complexity.

E. K-Fold Cross-Validation

K-Fold Cross-validation is a method of evaluating a machine learning model during training in which the dataset is partitioned into K subsets and the model is trained and assessed K times. The following image in Figure 6 shows how the K-fold works. The K-fold method utilized is stratified K-fold, which is a version of K-fold that returns stratified subsets [30]. Each of these subsets is formed by keeping a certain percentage of samples for each class.

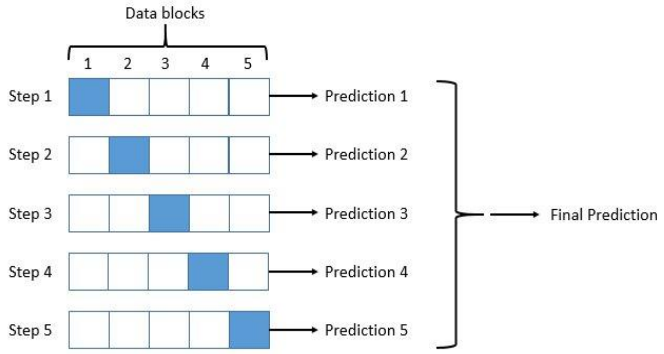

Figure 6. Illustration of K-fold

One of the subsets is chosen as the test set at each iteration, while the other K-1 subsets are utilized for training. This method has the advantage of utilizing data more efficiently, guaranteeing that the model does not overfit on a specific subset of data, and giving more consistent performance. Although it necessitates more processing resources and time, K-fold cross-validation is extremely beneficial for assessing models on relatively small datasets and assuring adequate generalization to previously untrained data.

F. Modeling Results

In a series of five K-fold evaluations, the results reveal that the model with gamma correction performs better than the model without such treatment. The CNN model on fold 1 had the greatest training score of 86.01, the CNN + gamma (-) model on fold 4 had a score of 91.38, and the CNN + gamma (+) model on fold 5 had a score of 89.72. It is worth noting that the best performance in each model was obtained at different folds, emphasizing the variety of evaluation findings in each K-fold iteration.

Table 1. Comparison of training model performance

Model	Accuracy of Fold					Average	
	1	2	3	4	5	Accuracy	Time (S)
CNN	**86,01**	78,09	85,31	84,38	84,58	83.67	13,39
CNN + Gamma (-)	89,98	88,11	87,41	**91,38**	84,35	88,25	12,99
CNN + Gamma (+)	86,95	89,28	83,45	86,71	**89,72**	87,22	13,45

After assessing K-fold five times, the conclusion in Table 1 indicates that the model with gamma correction performs better than the model without such treatment. The best CNN, CNN + gamma (-), and CNN + gamma (+) models got the greatest fold 1 (86.01), fold 4 (91.38), and fold 5 (89.72) scores, respectively.

ISSN:2302-8149
e-ISSN:2540-9719

Graph analysis can help you acquire a better understanding of model performance at each epoch and identify potential overfitting or underfitting. The amount of the lost value at each period may be shown in Figure 7. The lower the loss value, the higher the quality of the model being built.

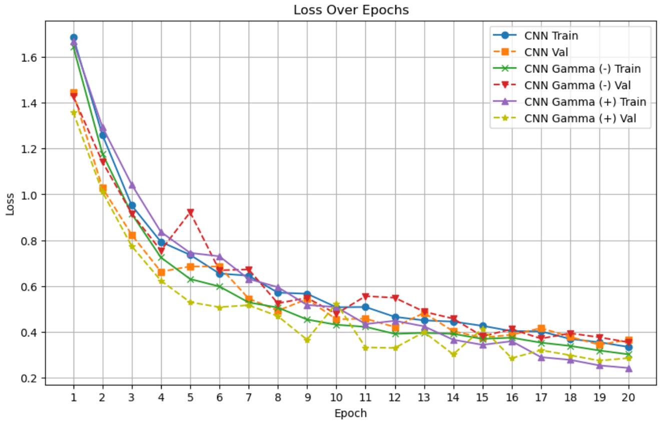

Figure 7. Loss graph per epoch

The graph depicts the model's loss outcomes, with final loss values of 0.33, 0.32, and 0.24 for training on the CNN, CNN gamma (-), and CNN gamma (+) models, respectively. Meanwhile, in the validation data, the loss values are 0.36, 0.35, and 0.29, respectively. The improved performance of the CNN+gamma combo demonstrates its capacity to lower loss values. Figure 8 will illustrate how the model was able to accurately predict the validation data at each epoch in the accuracy graph for the best model. This graphic analysis will give you an overview of the model's accuracy at each training step.

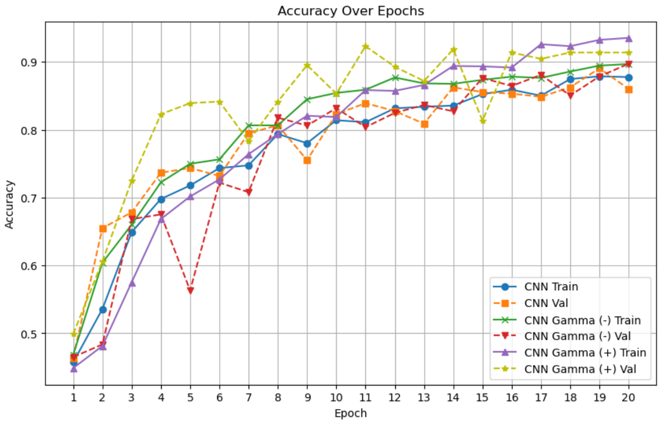

Figure 8. Accuracy graph for each epoch in the best model

Figure 8 shows that the CNN, CNN + gamma (-), and CNN + gamma (+) algorithms achieve accuracy values of 87.76, 89.68, and 93.53, respectively, on training data. Meanwhile, the accuracy values in the validation data were 86.01, 89.72, and 91.38. As a result, it is possible to conclude that using the CNN+gamma combination can increase accuracy performance when compared to models without gamma treatment. This demonstrates that incorporating gamma correction into the CNN model improves the model's capacity to produce accurate predictions, as evidenced by the increase in accuracy values on both data sets (training and validation).

G. Model Evaluation Results

A confusion matrix is used to evaluate models and offers information on classification performance in each class. This matrix can generate evaluation metrics including precision (equation 8), recall (equation 9), and specificity (equation 10). The matrix is used in this context to assess the model's ability to correctly categorize each class. These equations can be written down as follows:

$$Precision = \frac{TP}{TP + FP} \tag{8}$$

$$Sensitivity = \frac{TP}{TP + FN} \tag{9}$$

 ISSN:2302-8149
e-ISSN:2540-9719

$$Specificity = \frac{TN}{TN + FP} \qquad (10)$$

Using this matrix, it is possible to assess how well the model distinguishes between positive and negative classes, as well as how well the model properly identifies examples of each class. The true positives (TP), false positives (FP), true negatives (TN), and false negatives (FN) values in the confusion matrix represent the categorization results in each class. Table 2 displays the results of the confusion matrix.

Table 2. Comparison of testing model performance

Model	Accuracy	Precision	Sensitivity	Specificity
CNN	86.52	83.63	86.11	93.27
CNN + HE [18]	86. 30	84.91	83.68	93.52
CNN + Gamma (-)	88.59	87.59	86.68	94.17
CNN + Gamma (+)	88.80	86.49	88.06	94.50

The best model's confusion matrix image (CNN with gamma correction) can provide a visual assessment of the model's effectiveness in classifying events into positive and negative categories. With an increase of roughly 2%, this demonstrates that using gamma correction improves the model's classification accuracy.

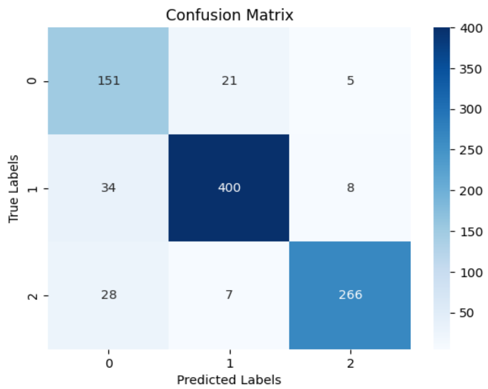

Figure 9. Confusion matrix value of the best model

Furthermore, the confusion matrix graph in Figure 9 can provide additional insight into the model's ability to distinguish between genuine positives, false positives, true negatives, and false negatives. An examination of these factors can provide a more in-depth insight into model performance in each classification class. Precision values can be calculated for the meningioma class (Class 0). Precision is computed by dividing the number of true positives (TP) by the number of false positives (FP). We can calculate recall if false negatives are provided. However, it should be emphasized that the information presented does not include true positives (TP), hence we do not have enough values to assess precision or recall directly. For a more thorough review, we need ideally have all elements of the confusion matrix (TP, FP, TN, FN) for each class. As a side note, accuracy is a metric that evaluates the proportion of positive instances categorized by the model that are genuinely positive. As a result, as stated in the conclusion, poorer precision can suggest the existence of classes with similar data to other classes.

5 Conclusion

Several conclusions can be drawn based on the results and analysis of the experiments, namely: the CNN model with gamma correction gave better results with values of 88.59% and 88.80% than CNN without gamma treatment, with values of 86.52%, by increasing the accuracy value by 2%. The technology suggested in this research can be developed and, in the future, utilized in the realm of medicine for recognizing brain cancers using MRI. There are still flaws in some methods that have a lot of room for development. This is medical research, so only strong performance scores are required.

ISSN:2302-8149
e-ISSN:2540-9719

However, it can be used as an input to reduce the amount of imbalanced data, which is still an issue in this study. You can also utilize an architecture like ImageNet to improve performance.

Reference

[1] A. Kabir Anaraki, M. Ayati, and F. Kazemi, "Magnetic resonance imaging-based brain tumor grades classification and grading via convolutional neural networks and genetic algorithms," *Biocybernetics and Biomedical Engineering*, vol. 39, no. 1, pp. 63–74, Jan. 2019, doi: 10.1016/j.bbe.2018.10.004.

[2] E. Wright *et al.*, "Incidentally found brain tumors in the pediatric population: a case series and proposed treatment algorithm," *J Neurooncol*, vol. 141, no. 2, pp. 355–361, Jan. 2019, doi: 10.1007/s11060-018-03039-1.

[3] W. Ayadi, W. Elhamzi, I. Charfi, and M. Atri, "A hybrid feature extraction approach for brain MRI classification based on Bag-of-words," *Biomedical Signal Processing and Control*, vol. 48, pp. 144–152, Feb. 2019, doi: 10.1016/j.bspc.2018.10.010.

[4] S. Kumar and D. P. Mankame, "Optimization driven Deep Convolution Neural Network for brain tumor classification," *Biocybernetics and Biomedical Engineering*, vol. 40, no. 3, pp. 1190–1204, Jul. 2020, doi: 10.1016/j.bbe.2020.05.009.

[5] R. Anitha and D. Siva Sundhara Raja, "Development of computer-aided approach for brain tumor detection using random forest classifier," *Int J Imaging Syst Tech*, vol. 28, no. 1, pp. 48–53, Mar. 2018, doi: 10.1002/ima.22255.

[6] E. Sert, F. Özyurt, and A. Doğantekin, "A new approach for brain tumor diagnosis system: Single image super resolution based maximum fuzzy entropy segmentation and convolutional neural network," *Medical Hypotheses*, vol. 133, p. 109413, Dec. 2019, doi: 10.1016/j.mehy.2019.109413.

[7] Universitas Dian Nuswantoro *et al.*, "New Workflow for Marine Fish Classification Based on Combination Features and CLAHE Enhancement Technique," *IJIES*, vol. 13, no. 4, pp. 293–304, Aug. 2020, doi: 10.22266/ijies2020.0831.26.

[8] B. Sekeroglu, "Time-shift image enhancement method," *Image and Vision Computing*, vol. 138, p. 104810, Oct. 2023, doi: 10.1016/j.imavis.2023.104810.

[9] F. Özyurt, E. Sert, E. Avci, and E. Dogantekin, "Brain tumor detection based on Convolutional Neural Network with neutrosophic expert maximum fuzzy sure entropy," *Measurement*, vol. 147, p. 106830, Dec. 2019, doi: 10.1016/j.measurement.2019.07.058.

[10] M. Angulakshmi and G. G. Lakshmi Priya, "Walsh Hadamard Transform for Simple Linear Iterative Clustering (SLIC) Superpixel Based Spectral Clustering of Multimodal MRI Brain Tumor Segmentation," *IRBM*, vol. 40, no. 5, pp. 253–262, Oct. 2019, doi: 10.1016/j.irbm.2019.04.005.

[11] A. Mittal and D. Kumar, "AiCNNs (Artificially-integrated Convolutional Neural Networks) for Brain Tumor Prediction," *EAI Endorsed Transactions on Pervasive Health and Technology*, vol. 5, no. 17, p. 161976, Feb. 2019, doi: 10.4108/eai.12-2-2019.161976.

[12] A. Wadhwa, A. Bhardwaj, and V. Singh Verma, "A review on brain tumor segmentation of MRI images," *Magnetic Resonance Imaging*, vol. 61, pp. 247–259, Sep. 2019, doi: 10.1016/j.mri.2019.05.043.

[13] J. Chang *et al.*, "A mix-pooling CNN architecture with FCRF for brain tumor segmentation," *Journal of Visual Communication and Image Representation*, vol. 58, pp. 316–322, Jan. 2019, doi: 10.1016/j.jvcir.2018.11.047.

[14]J. Amin, M. Sharif, N. Gul, M. Yasmin, and S. A. Shad, "Brain tumor classification based on DWT fusion of MRI sequences using convolutional neural network," *Pattern Recognition Letters*, vol. 129, pp. 115–122, Jan. 2020, doi: 10.1016/j.patrec.2019.11.016.

[15]T. Saba, A. Sameh Mohamed, M. El-Affendi, J. Amin, and M. Sharif, "Brain tumor detection using fusion of hand crafted and deep learning features," *Cognitive Systems Research*, vol. 59, pp. 221–230, Jan. 2020, doi: 10.1016/j.cogsys.2019.09.007.

[16]S. Lu, Z. Lu, and Y.-D. Zhang, "Pathological brain detection based on AlexNet and transfer learning," *Journal of Computational Science*, vol. 30, pp. 41–47, Jan. 2019, doi: 10.1016/j.jocs.2018.11.008.

[17]M. Sajjad, S. Khan, K. Muhammad, W. Wu, A. Ullah, and S. W. Baik, "Multi-grade brain tumor classification using deep CNN with extensive data augmentation," *Journal of Computational Science*, vol. 30, pp. 174–182, Jan. 2019, doi: 10.1016/j.jocs.2018.12.003.

[18]S. Saifullah and R. Dreżewski, "Modified Histogram Equalization for Improved CNN Medical Image Segmentation," *Procedia Computer Science*, vol. 225, pp. 3021–3030, 2023, doi: 10.1016/j.procs.2023.10.295.

[19]M. Naufal, H. Al Azies, G. A. Firmansyah, and N. M. K. Kharisma, "Penerapan teknik adaptive dan histogram equalization dalam pengolahan citra," *IlmuKomputer*, vol. 5, no. 1, pp. 9–18, Mar. 2024, doi: 10.24127/ilmukomputer.v5i1.5345.

[20]M. Hayati *et al.*, "Impact of CLAHE-based image enhancement for diabetic retinopathy classification through deep learning," *Procedia Computer Science*, vol. 216, pp. 57–66, 2023, doi: 10.1016/j.procs.2022.12.111.

[21]R. K. Sidhu, J. Sachdeva, and D. Katoch, "Segmentation of retinal blood vessels by a novel hybrid technique- Principal Component Analysis (PCA) and Contrast Limited Adaptive Histogram Equalization (CLAHE)," *Microvascular Research*, vol. 148, p. 104477, Jul. 2023, doi: 10.1016/j.mvr.2023.104477.

[22]I. S. Chandra, R. K. Shastri, D. Kavitha, K. R. Kumar, S. Manochitra, and P. B. Babu, "CNN based color balancing and denoising technique for underwater images: CNN-CBDT," *Measurement: Sensors*, vol. 28, p. 100835, Aug. 2023, doi: 10.1016/j.measen.2023.100835.

[23]Q. Wang, Z. Li, S. Zhang, N. Chi, and Q. Dai, "A versatile Wavelet-Enhanced CNN-Transformer for improved fluorescence microscopy image restoration," *Neural Networks*, vol. 170, pp. 227–241, Feb. 2024, doi: 10.1016/j.neunet.2023.11.039.

[24]R. Maurya and S. Wadhwani, "An Efficient Method for Brain Image Preprocessing with Anisotropic Diffusion Filter & Tumor Segmentation," *Optik*, vol. 265, p. 169474, Sep. 2022, doi: 10.1016/j.ijleo.2022.169474.

[25]F. Lin, H. Zhang, J. Wang, and J. Wang, "Unsupervised image enhancement under non-uniform illumination based on paired CNNs," *Neural Networks*, vol. 170, pp. 202–214, Feb. 2024, doi: 10.1016/j.neunet.2023.11.014.

[26]M. Veluchamy and B. Subramani, "Image contrast and color enhancement using adaptive gamma correction and histogram equalization," *Optik*, vol. 183, pp. 329–337, Apr. 2019, doi: 10.1016/j.ijleo.2019.02.054.

[27]"Figshare brain tumor dataset." doi: 10.6084/m9.figshare.1512427.v5.

[28] A. Kumar Sahoo, P. Parida, K. Muralibabu, and S. Dash, “Efficient simultaneous segmentation and classification of brain tumors from MRI scans using deep learning,” *Biocybernetics and Biomedical Engineering*, vol. 43, no. 3, pp. 616–633, Jul. 2023, doi: 10.1016/j.bbe.2023.08.003.

[29] M. Celik and O. Inik, “Development of hybrid models based on deep learning and optimized machine learning algorithms for brain tumor Multi-Classification,” *Expert Systems with Applications*, vol. 238, p. 122159, Mar. 2024, doi: 10.1016/j.eswa.2023.122159.

[30] Muljono, Pulung Nurtantio Andono, Sari Ayu Wulandari, Harun Al Azies, and Muhammad Naufal, “Tempo Recognition of Kendhang Instruments Using Hybrid Feature Extraction,” vol. 27, no. 3, Mar. 2024, doi: 10.6180/jase.202403_27(3).0004.